Immunoavidity-based Capture of Tumor Exosomes using Poly(amidoamine) Dendrimer Surfaces

Michael J. Poellmann¹, Ashita Nair¹, Jiyoon Bu¹, Jack K. H. Kim¹, Randall J. Kimple^{2,3}, and Seungpyo Hong^{1,3,4,5}*

¹Pharmaceutical Sciences Division, School of Pharmacy, University of Wisconsin-Madison, WI 53705

²Department of Human Oncology, School of Medicine and Public Health, University of Wisconsin-Madison, WI 53705

³Carbone Cancer Center, University of Wisconsin-Madison, WI 53705

⁴Department of Biomedical Engineering, University of Wisconsin-Madison, WI 53706

⁵Yonsei Frontier Lab and Department of Pharmacy, Yonsei University, Seoul, KOREA 03722

*Address all correspondence to:

Prof. Seungpyo Hong
Pharmaceutical Sciences Division, School of Pharmacy
University of Wisconsin – Madison
7121 Rennebohm Hall
777 Highland Avenue
Madison, WI 53705, USA
email: seungpyo.hong@wisc.edu
phone: (608) 890-0699

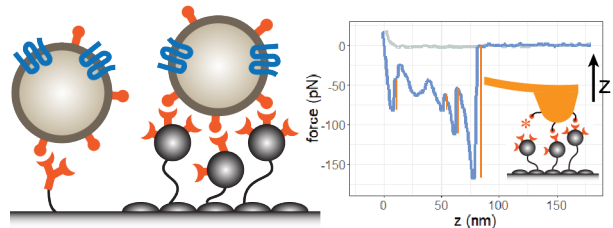
KEYWORDS

exosome, extracellular vesicle, multivalent binding, poly(amidoamine) dendrimer, biomarker

ABSTRACT

Tumor-derived blood-circulating exosomes have potential as a biomarker to greatly improve cancer treatment. However, effective isolation of exosomes remains a tremendous technical challenge. This study presents a novel nanostructured polymer surface for highly effective capture of exosomes through strong avidity. Various surface configurations, consisting of multivalent dendrimers, PEG, and tumor-targeting antibodies, were tested using exosomes isolated from tumor cell lines. We found that a dual layer dendrimer configuration exhibited the highest efficiency in capturing cultured exosomes spiked into human serum. Importantly, the optimized surface captured a >4-fold greater amount of tumor exosomes from head and neck cancer patient plasma samples than that from healthy donors. Nanomechanical analysis using atomic force microscopy also revealed that the enhancement was attributed to multivalent binding (avidity) and augmented short-range adhesion mediated by dendrimers. Our results support that the dendrimer surface detects tumor exosomes at high sensitivity and specificity, demonstrating its potential as a new cancer liquid biopsy platform.

TABLE OF CONTENTS FIGURE



enhanced immunoavidity capture through dendrimermediated multivalent and short range interactions

MAIN TEXT

New technologies for the diagnosis and prognosis of cancer will drive the practice of precision medicine. Liquid biopsies are primed to be such a technology because they are minimally invasive and can be frequently performed through simple blood-draw. The tests are designed to detect biomarkers, such as cell free DNA (cfDNA), circulating tumor cells (CTCs), or extracellular vesicles (EVs) including exosomes, that tumors regularly shed into the blood¹. Although the greatest amount of information could be derived from CTCs among the biomarkers, the cells are exceptionally rare and heterogeneous in phenotype², making clinically significant detection and analysis difficult. In contrast, cfDNA is relatively easy to be detected in blood due to its abundance, however, it fails to offer dynamic information regarding changes in gene expression³. Exosomes, being positioned between these two more explored biomarkers in terms of size, abundance, and potential diagnostic information, represent an emerging class of cancer biomarkers found in blood. These nanoscale vesicles contain functional mRNA packaged within a membrane that carries the same characteristic surface markers as the cell they originated from⁴⁻⁵. Furthermore, existing literature has linked the composition and release rate of exosomes

to malignancy and metastasis⁶⁻⁸, demonstrating the great potential of these vesicles as prognostic biomarkers.

The current gold-standard technique to isolate exosomes from blood is ultracentrifugation that is slow, difficult to use, and nonspecific⁹. Other commercially available methods include precipitation and size-based filtration techniques, such as ExoQuick® and ExospinTM. However, each of these methods suffers from a lack of specificity towards tumor-derived exosomes. Instead, immunoaffinity-based approaches could offer such selectivity, in addition to high sensitivity and better sample preservation¹⁰⁻¹¹. Immunoaffinity techniques employ exosome- or cancer-targeting antibodies typically on the surfaces of magnetic beads ¹²⁻¹³ or into microfluidic channels¹⁴⁻¹⁹. These immunoaffinity-based methods, however, rely entirely on the binding affinity of capture antibodies, which have yet to make significant clinical impact likely due to their insufficient sensitivity and specificity.

We hypothesized that the sensitivity and specificity of exosome immunoaffinity devices could be substantially enhanced with a nanostructured polymer surface that mediates binding avidity through multivalent immunorecognition²⁰. Our previously-reported liquid biopsy device for CTCs was based, in part, on a surface coated with poly(amidoamine) (PAMAM) dendrimers that effectively mediated multivalent binding effect (avidity), resulting in improved capture efficiency for CTCs²¹⁻²⁴. These flexible, hyperbranched nanoparticles facilitate multivalent capture in two ways: a high density of functional groups allows for multiple antibodies to be attached to each ~9 nm dendrimer; and the structure is deformable enough to accommodate reorientation of binding domains²². However, exosomes are 1/100th the diameter of CTCs. The smaller dimensions necessitated the development of a new capture surface to achieve multivalent binding (avidity)-based capture at this nanoscale.

In this study, our exosome capture surface contained three layers of polymers designed to minimize nonspecific binding while providing multivalency and a high degree of flexibility for antibody orientation. First, an epoxide-functionalized glass slide was coated with partially carboxylated, generation 7 (G7) PAMAM dendrimers (see **Figure S1** for ¹H NMR confirmation)²². Next, a mixture of poly(ethylene glycol) (PEG) was conjugated to the dendrimers and any remaining epoxide groups. The PEG mixture consisted of heterobifunctional PEG tethers with molecular weight (MW) of 5 and 20 kDa for conjugation with another layer of dendrimers and 2 kDa methoxy-PEG (mPEG) to block nonspecific adsorption. Finally, the tethers were topped with a second layer of carboxylated PAMAM dendrimers, resulting in a two-layer dendrimer surface. **Figure 1** illustrates the relative configurations of controls, consisting of PEG tethers alone, our previous CTC capture (single layer dendrimer) surface, and the dual layer dendrimer surface described here.

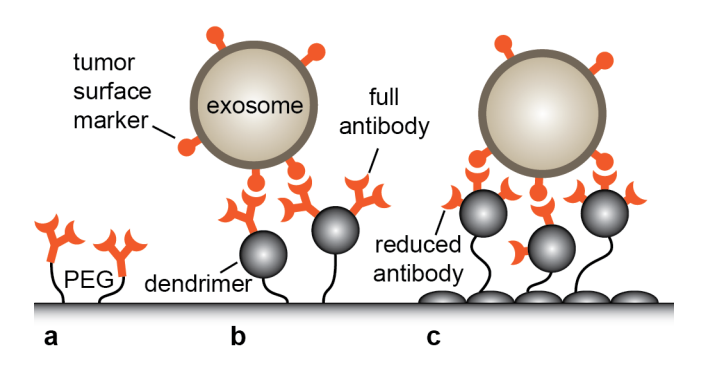


Figure 1. Illustration of capture surface configurations tested in this study. PEG tethers are indicated by black lines and G7 PAMAM dendrimers by gray circles. a) PEG-tethered antibodies against tumor cell surface markers. b) Full antibodies on a single layer dendrimer surface, equivalent to our previously-reported CTC capture device. c) Reduced antibodies on a dual layer dendrimer surface, shown here to support multivalent capture on the nanoscale.

Sessile drop contact angle measurements provided confirmation that each successive layer of polymer resulted in a more hydrophilic surface (Figure 2a, Figure S2). Surface topography was visualized using non-contact mode atomic force microscopy (AFM) (see Figure 2b for the dual layer dendrimer surface and Figure S3 for other surface configurations). The surface roughness of the various configurations was also measured using AFM (Figure 2c, Figure S3), revealing the root mean square (Rq) value of 2.5 nm for the dual layer dendrimer surface, which was significantly greater than all other surface configurations (p < .05). Note that the true feature size may not have been fully resolved by this method, as the Flory radius of 20 kDa PEG tether is over 13 nm²⁵. Nevertheless, the measured roughness values increased as each polymer layer was added and are consistent with previously-reported dimensions for surfaceadsorbed PAMAM dendrimers²⁶. In addition, single and dual layer configurations were treated with the same number of fluorescently labelled antibodies (rhodamine-conjugated anti-epithelial adhesion molecule (aEpCAM), a commonly used protein for CTC capture). As shown in Figure **S4**, the measured fluorescence intensities were increased as each layer was added to the surfaces. The immobilized antibody density was calculated to have an equivalent of over 1,000 binding sites per µm², which is sufficiently high to mediate multivalent binding between exosomes and the capture surface (see Supplementary Information for assumptions). The decreased contact angles, increased surface roughness, and increased antibody fluorescence all confirmed the successful layer-by-layer surface functionalization.

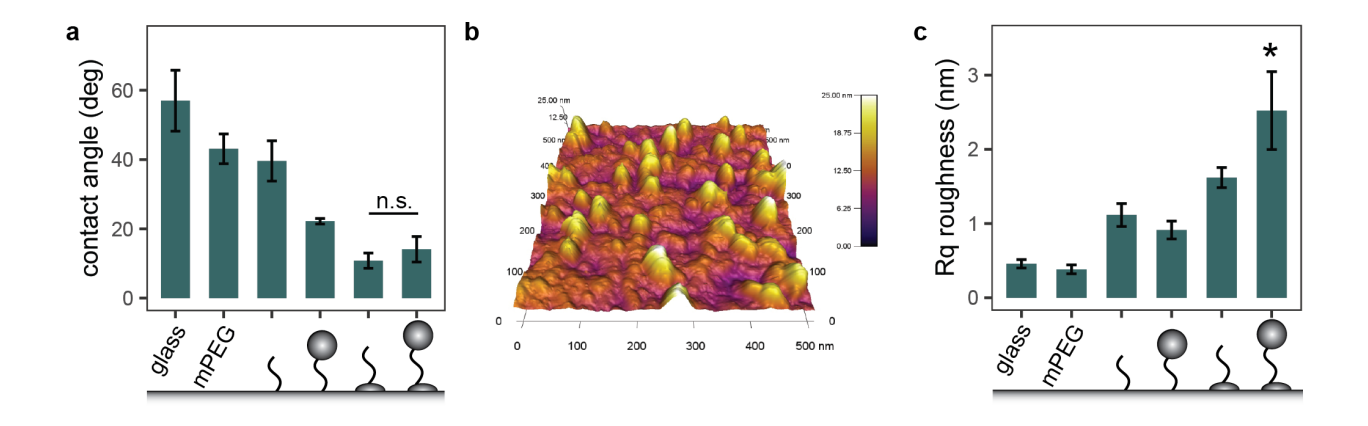


Figure 2. Surface characterization of various polymer configurations. a) The contact angles decreased with addition of PEG or dendrimers, indicating increased hydrophilicity of the surfaces upon polymer coating (n = 8). b) Stylized rendering of nanoscale features on the dual layer dendrimer surface imaged with non-contact AFM. c) Significantly greater roughness of dual layer dendrimer surfaces compared to all other polymer configurations (n = 3, p < .05).

To compare the various surface configurations in terms of tumor exosome capture efficiency, the surfaces were functionalized with aEpCAM (full antibody) and incubated with MCF-7 cell-derived exosomes stained with green fluorescent Vybrant™ DiO, as depicted in **Figure 3a**. In parallel, we also tested the functionality of reduced (partial) antibodies of aEpCAM that were cleaved at the disulfide bonds between heavy chains² and subsequently conjugated to dendrimers through the exposed sulfhydryl groups. Compared to full antibodies, the partially reduced antibodies have smaller size that may enhance conformational flexibility, while conjugation to sulfhydryl groups may result in a more consistent outward orientation of binding sites²8. **Figure 3b** shows enhanced capture on dual layer surfaces compared to antibodies (for both full and reduced) conjugated to bare glass, PEG, or single layer dendrimer surfaces (p < .001). In particular, the fluorescence signal was 5.5-fold higher on the dual layer dendrimer surfaces with reduced aEpCAM, compared to the glass surfaces with full aEpCAM. Although we did not observe statistically significant differences between the same surface

configurations with reduced vs. full antibodies (p = .212), mean capture on the surfaces with reduced aEpCAM was consistently higher than those with full aEpCAM. Considering this capture improvement and the advantages of reduced antibodies mentioned above, we used reduced antibodies going forward.

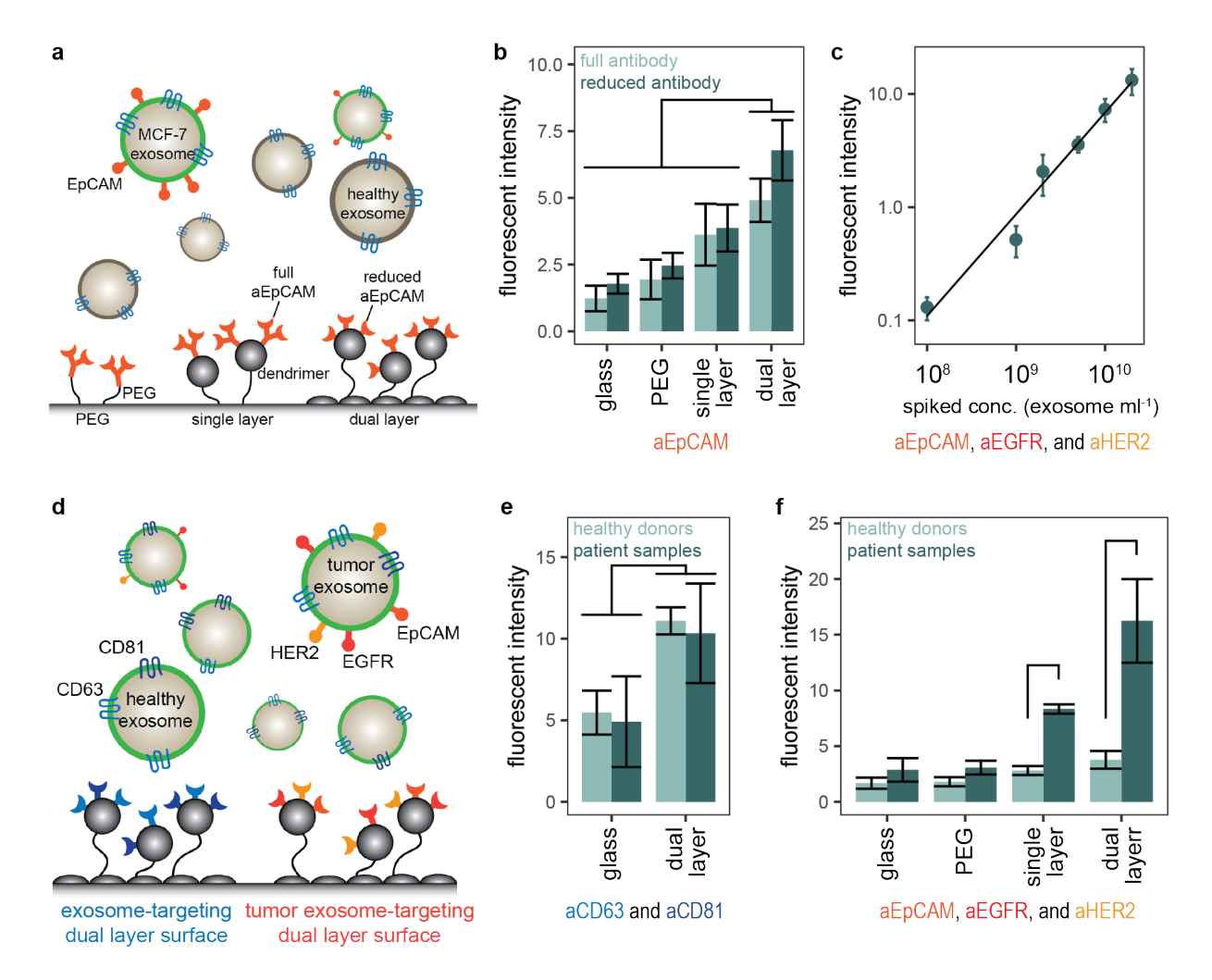


Figure 3. Evaluation of exosome capture on various polymer surfaces engineered to achieve binding avidity. a) Various surfaces to compare their capture of exosomes derived from cell cultures after being labeled with a lipophilic green fluorescent dye (VybrantTM DiO) and spiked into healthy human serum. b) Dual layer dendrimer surfaces functionalized with anti-EpCAM exhibiting enhanced capture of MCF-7-derived exosomes, compared to all other surface configurations (n = 6, p < .05) with both full and reduced antibodies. c) MDA-MB-231 cell-derived exosome capture on the dual layer dendrimer surfaces functionalized with three antibodies, aEpCAM, aEGFR, and aHER2, showing the linearity of fluorescence signals in the range of concentrations (n = 5, $R^2 = .994$). d) Illustration of surface capture of VybrantTM DiO-labelled exosomes in blood collected from five HNSCC patients and three healthy donors. e) Enhanced

capture by the dual layer dendrimer surfaces functionalized with exosome-targeting antibodies against CD63 and CD81 in both groups (p = .037). f) Significantly enhanced sensitivity and specificity of the tumor exosome-targeting dendrimer surfaces in detecting tumor exosomes from HNSCC patient samples (p = .027). All plots show mean \pm -standard error.

We then employed a mixture of three tumor-targeting antibodies to further improve the capture of tumor exosomes. As we reported previously, relying on a single tumor-specific antibody, mostly aEpCAM, is not sufficient to capture circulating biomarkers such as CTCs, considering that many tumor biomarkers undergo the phenotypic changes often losing expression of EpCAM²¹. To address this, we previously reported that dendrimer surfaces coated with a mixture of antibodies targeting epithelial cell adhesion molecule (EpCAM), epidermal growth factor receptor (EGFR), and human epidermal growth factor receptor 2 (HER2) were highly effective in capturing CTCs in blood samples drawn from patients with head and neck squamous cell carcinoma (HNSCC) and other cohorts^{24, 29}. We thus used the same antibodies in this study to selectively capture tumor-derived exosomes on our exosome capture surfaces. Exosomes derived from MDA-MB-231 cells that express all three proteins³⁰⁻³¹ were also employed due to the fact that MCF-7 do not express a high level of HER2²¹. Note that the EVs from the both cell lines were confirmed to be <160 nm in diameter (**Table S1**) and express tetraspanins that are characteristics of exosomes (**Figure S5**). The cultured exosomes were labeled with Vybrant™ DiO and spiked into healthy human serum at varying concentrations. We observed a nearlylinear relationship ($R^2 = 0.994$) of fluorescence intensity with spiked exosome concentration ranging from 108 to 2x1010 exosomes per mL of plasma (Figure 3c), which well covers the physiological/pathological range (typically 10⁹ vesicles mL⁻¹ of plasma from healthy individuals)³². All of these results indicated that our optimized capture surface would likely capture clinical tumor exosomes in a reliable manner.

Finally, we conducted a clinical pilot study with blood drawn from 5 HNSCC patients and 3 healthy donors, by performing experiments as illustrated in **Figure 3d**. To verify that our capture surfaces are specific to tumor exosomes, we first prepared control surfaces functionalized with aCD63 and aCD81 that target exosomes in general. As shown in **Figure 3e**, enhanced capture on the dual layer dendrimer surfaces was observed, compared to glass (p = .037), without noticeable differences between the plasma samples from the HNSCC patients and healthy controls. In sharp contrast, we observed dramatic differences in signal between patient and healthy donor samples when the dendrimer surfaces were coated with the three antibodies (aEpCAM, aEGFR, and aHER2) (Figure 3f). The glass and PEG surfaces were statistically unable to distinguish between patient and healthy donor samples. The single layer dendrimer surfaces exhibited 3-fold higher fluorescent signal from the patient blood than the healthy donor samples (p < .001). Remarkably, the dual layer dendrimer surfaces detected a 4.3-fold higher amount of tumor exosomes from the patient samples than that from the healthy donor samples (p = .027). Our results using the clinical samples continued to show enhanced capture on the dual layer surfaces compared to a single layer of dendrimers (p = .037). The difference may be attributed to a combination of ~9.4% greater binding site density (which did not reach statistical significance), increased wettability, and increased nanostructural complexity of the dual layer dendrimer surface.

The significant enhancement observed from the dual layer dendrimer surfaces in capturing exosomes from both cell lines and clinical blood plasma samples led us to investigate further to obtain mechanistic insight. We used AFM force spectroscopy to quantitatively measure the nanoscale interactions between exosomes and our capture surfaces. This technique is sensitive enough to detect the forces of antibody-antigen unbinding³³⁻³⁴, and has been used to

resolve multivalent unbinding events between ligand-functionalized dendrimers and surface-immobilized proteins³⁵. Note that the nominal diameter of the TR400PB AFM probe (Oxford Instruments) was around 60 nm, or approximately the scale of a single exosome. A probe was functionalized with PEG tethers and recombinant human EpCAM and used to represent an exosome. This probe was retracted from four surface configurations a minimum of 70 times, with no more than 15 curves collected at a single spot. To ensure that the probe did not degrade during evaluation, data were collected from the functionalized, dual layer dendrimer surface in the first and final rounds with no statistical degradation in maximum adhesion force (p = .73) or energy (p = .33). The experimental workflow is depicted in **Figure S6**, and representative force curves from the dual layer dendrimer surfaces are shown in **Figure 4a-c** with specific unbinding events annotated by vertical lines.

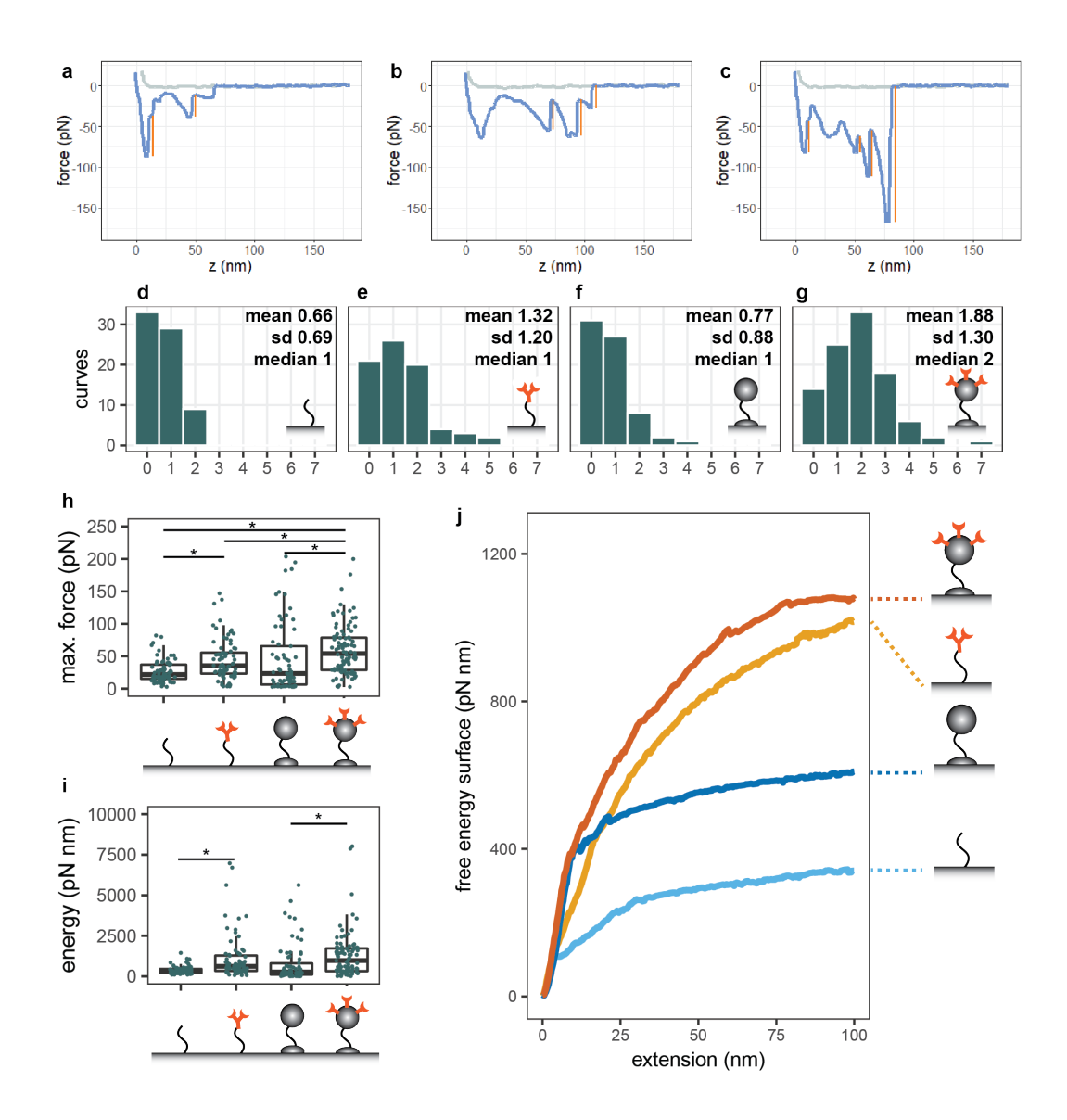


Figure 4. Characterization of binding avidity using AFM force spectroscopy. Example force curves from dual layer dendrimer capture surfaces functionalized with aEpCAM exhibiting a) two, b) three, and c) four distinct unbinding events. Histograms depict the number of distinct unbinding events in each retraction curve on d) nonfunctionalized PEG, e) PEG with full aEpCAM, f) nonfunctionalized dual layer dendrimer, and g) dual layer dendrimer functionalized with reduced aEpCAM. h) Maximum adhesion force and i) adhesion energy (work). Statistically significant differences at p < .05 are indicated by *. j) Free energy profiles calculated from the ensemble average of work-distance plots show enhanced adhesion by dual layer dendrimer surfaces without antibodies at distances < 10 nm.

Multivalent binding was quantified by counting the number of discrete unbinding events, identified as abrupt changes in the unloading force. A threshold of 16 pN was chosen to identify "specific" rupture events likely to be the result of antibody unbinding. This value was greater than ten times the root mean square of signal when the probe was far from the surface, ensuring that such events were not the product of random noise. Only the functionalized, dual layer dendrimer surfaces exhibited a median number of rupture events at 2 whereas all other surfaces showed 1 (**Figure 4d-g**). A mean of 1.88 unbinding events was observed per curve on the dual layer dendrimer surface (**Figure 4g**), compared to just 1.32 events on PEG with full antibodies (**Figure 4e**) (p < .05). Although unbinding events were observed on non-functionalized surfaces, a majority of retraction curves did not feature any rupture events.

The maximum adhesion force (**Figure 4h**) and energy of adhesion (**Figure 4i**) were also measured at the highest on the functionalized, dual layer dendrimer surfaces. Energy (estimated from the work of probe retraction) was calculated from the cumulative force times distance of separation. The maximum adhesive force on the dual layer dendrimer surfaces was a mean of 59.3 pN (standard deviation 37.9) compared to 43.9 pN (standard deviation 31.6) on PEG with full antibodies (p < .05). Similarly, the total energy of adhesion averaged 1,256 pN nm (standard deviation 1,346) on dual layer dendrimer compared to 1,110 pN nm (standard deviation 1,384) on the PEG controls. Surprisingly, non-functionalized dual layer dendrimer (without antibodies) had adhesive forces statistically similar to functionalized PEG (p = .27), although adhesive energy was lower (p < .05). This was unanticipated, given low levels of nonspecific binding observed in assays. The free energy profile for unbinding from each surface was reconstructed from the ensemble average of work-distance plots according to the method of Hummer and Szabo³⁶ (**Figure 4j**). The profile for both dual layer dendrimer surfaces (with and without

antibodies) displayed a similar slope below 10 nm extension, whereas they diverged beyond 10 nm. The profile for PEG surfaces functionalized with full antibodies surpassed the free energy of unfunctionalized, dual layer dendrimers at approximately 20 nm extension.

The AFM results revealed two separate mechanisms of exosome capture on dendrimer surfaces. First, dendrimers provided a high density of binding sites for binding exosomes far (>20 nm) above the surface. The use of reduced antibodies compared to full antibodies further contributes to multivalent recognition at sub-100 nm length scales. Once captured, dendrimers additionally contribute to short-range (<10 nm) adhesion. Similar, "nonspecific" interactions between dendrimers and proteins have been previously reported in AFM experiments and attributed to a combination of electrostatic and van der Waals forces ³⁷.

In conclusion, our results show that the nanostructured, dual layer dendrimer surface configuration achieves significantly enhanced capture of exosomes through multivalent binding effect. Compared to our previous CTC capture surface, this study demonstrated that a second layer of dendrimers significantly improve binding avidity at the nanoscale, enabling highly effective capture of tumor exosomes from both cell cultures and blood samples from HNSCC patients. We also provided mechanistic insight into the nanoscale phenomena responsible for enhanced capture by quantitatively measuring binding forces using AFM. Although further development and optimization is necessary for this capture surface to be routinely used in the clinic, the results suggest that dendrimer surfaces can greatly enhance detection of exosomes and other nanoscale biomarkers in blood plasma through exploiting strong binding avidity. The successful development of such biomarkers for liquid biopsy would ultimately contribute the realization of precision medicine.

ASSOCIATED CONTENT

Supporting Information Supporting information contains supplementary methods, results, and

figures. This material is available free of charge via the Internet at http://pubs.acs.org

AUTHOR INFORMATION

Corresponding Author

*Address all correspondence to:

Prof. Seungpyo Hong Pharmaceutical Sciences Division, School of Pharmacy University of Wisconsin – Madison 7121 Rennebohm Hall 777 Highland Avenue

Madison, WI 53705, USA

 $email: \underline{seungpyo.hong@wisc.edu}\\$

phone: (608) 890-0699

Author Contributions

MJP and SH conceptualized the project and wrote the manuscript. MJP, AN, and JKHK

conducted the experiments. MJP, AN, JB, and SH designed the experiments and conducted the

data analysis. All authors have given approval to the final version of the manuscript.

15

Funding Sources

Portions of this work were funded by the National Science Foundation (NSF) under grant #DMR-1808251, the National Cancer Institute, National Institutes of Health (NCI/NIH) through grant #1R01CA182528, and University of Wisconsin intramural funds. Instrumentation at the Materials Science Center was funded by University of Wisconsin-Madison College of Engineering Shared Research Facilities and NSF through DMR-1720415.

Conflict of Interest

MJP and SH are associated with Capio Biosciences, Inc., a biotech startup developing biomarkers for liquid biopsy, where SH is a co-founder and has a significant equity share.

ACKNOWLEDGEMENT

The authors would like to thank Vedant Bodke (UW-Madison) and Juae Kim (Ewha Womens University) for assistance in preparing experiments. Contact angle measurements were collected at the UW-Madison Materials Science Center.

ABBREVIATIONS

AFM, atomic force microscope; cfDNA, cell-free deoxyribonucleic acid; CTC, circulating tumor cell; EGFR, epidermal growth factor receptor; ELISA, enzyme-linked immunoadsorbant assay;

EpCAM, epithelial cell adhesion molecule; EV, extracellular vesicle; G7, generation 7; HER2, human epidermal growth factor receptor 2; mPEG, methoxy poly(ethylene glycol); mRNA, messenger ribonucleic acid; PAMAM, poly(amidoamine); PEG, poly(ethylene glycol); SMCC, succinimidyl-trans-4-(N-maleimidylmethyl)cyclohexane-1-carboxylate.

REFERENCES

- 1. Alix-Panabieres, C.; Pantel, K., Clinical applications of circulating tumor cells and circulating tumor DNA as liquid biopsy. *Cancer Discovery* **2016**, *6* (5), 479-91.
- 2. Myung, J. H.; Park, S. J.; Wang, A. Z.; Hong, S., Integration of biomimicry and nanotechnology for significantly improved detection of circulating tumor cells (CTCs). *Advanced Drug Delivery Reviews* **2018**, *125*, 36-47.
- 3. Moon, D. H.; Lindsay, D. P.; Hong, S.; Wang, A. Z., Clinical indications for, and the future of, circulating tumor cells. *Advanced Drug Delivery Reviews* **2018**, *125*, 143-150.
- 4. Colombo, M.; Raposo, G.; Thery, C., Biogenesis, secretion, and intercellular interactions of exosomes and other extracellular vesicles. *Annual Review of Cell and Developmental Biology* **2014**, *30*, 255-89.
- 5. Maas, S. L. N.; Breakefield, X. O.; Weaver, A. M., Extracellular vesicles: unique intercellular delivery vehicles. *Trends in Cell Biology* **2017**, *27* (3), 172-188.
- 6. Azmi, A. S.; Bao, B.; Sarkar, F. H., Exosomes in cancer development, metastasis, and drug resistance: a comprehensive review. *Cancer Metastasis Reviews* **2013**, *32* (3-4), 623-42.
- 7. Milane, L.; Singh, A.; Mattheolabakis, G.; Suresh, M.; Amiji, M. M., Exosome mediated communication within the tumor microenvironment. *Journal of Controlled Release* **2015**, *219*, 278-294.
- 8. Syn, N.; Wang, L.; Sethi, G.; Thiery, J. P.; Goh, B. C., Exosome-mediated metastasis: from epithelial-mesenchymal transition to escape from immunosurveillance. *Trends in Pharmacological Sciences* **2016**, *37* (7), 606-617.
- 9. Contreras-Naranjo, J. C.; Wu Hj Fau Ugaz, V. M.; Ugaz, V. M., Microfluidics for exosome isolation and analysis: enabling liquid biopsy for personalized medicine. *Lab on a Chip* **2017**, *17* (21), 3558-3577.
- 10. Liga, A.; Vliegenthart, A. D.; Oosthuyzen, W.; Dear, J. W.; Kersaudy-Kerhoas, M., Exosome isolation: a microfluidic road-map. *Lab on a Chip* **2015**, *15* (11), 2388-94.
- 11. Li, P.; Kaslan, M.; Lee, S. H.; Yao, J.; Gao, Z., Progress in exosome isolation techniques. *Theranostics* **2017**, *7* (3), 789-804.
- 12. He, M.; Crow, J.; Roth, M.; Zeng, Y.; Godwin, A. K., Integrated immunoisolation and protein analysis of circulating exosomes using microfluidic technology. *Lab on a Chip* **2014**, *14* (19), 3773-80.
- 13. Zhao, Z.; Yang, Y.; Zeng, Y.; He, M., A microfluidic ExoSearch chip for multiplexed exosome detection towards blood-based ovarian cancer diagnosis. *Lab on a Chip* **2016**, *16* (3), 489-96.
- 14. Chen, C.; Skog, J.; Hsu, C. H.; Lessard, R. T.; Balaj, L.; Wurdinger, T.; Carter, B. S.; Breakefield, X. O.; Toner, M.; Irimia, D., Microfluidic isolation and transcriptome analysis of serum microvesicles. *Lab on a Chip* **2010**, *10* (4), 505-11.
- 15. Kanwar, S. S.; Dunlay, C. J.; Simeone, D. M.; Nagrath, S., Microfluidic device (ExoChip) for on-chip isolation, quantification and characterization of circulating exosomes. *Lab on a Chip* **2014**, *14* (11), 1891-900.
- 16. Chen, C.; Lin, B. R.; Hsu, M. Y.; Cheng, C. M., Paper-based devices for isolation and characterization of extracellular vesicles. *Journal of Visualized Experiments: JoVE* **2015**, (98), e52722.

- 17. Hisey, C. L.; Dorayappan, K. D. P.; Cohn, D. E.; Selvendiran, K.; Hansford, D. J., Microfluidic affinity separation chip for selective capture and release of label-free ovarian cancer exosomes. *Lab on a Chip* **2018**, *18* (20), 3144-3153.
- 18. Zhang, P.; Zhou, X.; He, M.; Shang, Y.; Tetlow, A. L.; Godwin, A. K.; Zeng, Y., Ultrasensitive detection of circulating exosomes with a 3D-nanopatterned microfluidic chip. *Nature Biomedical Engineering* **2019**.
- 19. Reategui, E.; van der Vos, K. E.; Lai, C. P.; Zeinali, M.; Atai, N. A.; Aldikacti, B.; Floyd, F. P., Jr.; A, H. K.; Thapar, V.; Hochberg, F. H.; Sequist, L. V.; Nahed, B. V.; B, S. C.; Toner, M.; Balaj, L.; D, T. T.; Breakefield, X. O.; Stott, S. L., Engineered nanointerfaces for microfluidic isolation and molecular profiling of tumor-specific extracellular vesicles. *Nature Communications* **2018**, *9* (1), 175.
- 20. Krishnamurthy, V. M.; Estroff, L. A.; Whitesides, G. M., Multivalency in Ligand Design. In *Fragment-based Approaches in Drug Discovery*, Jahnke, W.; Erlanson, D. A., Eds. Wiley-VCH Verlag GmbH & Co: 2006.
- 21. Myung, J. H.; Gajjar, K. A.; Chen, J.; Molokie, R. E.; Hong, S., Differential detection of tumor cells using a combination of cell rolling, multivalent binding, and multiple antibodies. *Analytical Chemistry* **2014**, *86* (12), 6088-94.
- 22. Myung, J. H.; Gajjar, K. A.; Saric, J.; Eddington, D. T.; Hong, S., Dendrimer-mediated multivalent binding for the enhanced capture of tumor cells. *Angewandte Chemie (International ed. in English)* **2011**, *50* (49), 11769-72.
- 23. Myung, J. H.; Roengvoraphoj, M.; Tam, K. A.; Ma, T.; Memoli, V. A.; Dmitrovsky, E.; Freemantle, S. J.; Hong, S., Effective capture of circulating tumor cells from a transgenic mouse lung cancer model using dendrimer surfaces immobilized with anti-EGFR. *Analytical Chemistry* **2015**, *87* (19), 10096-102.
- 24. Myung, J. H.; Eblan, M. J.; Caster, J. M.; Park, S. J.; Poellmann, M. J.; Wang, K.; Tam, K. A.; Miller, S. M.; Shen, C.; Chen, R. C.; Zhang, T.; Tepper, J. E.; Chera, B. S.; Wang, A. Z.; Hong, S., Multivalent binding and biomimetic cell rolling improves the sensitivity and specificity of circulating tumor cell capture. *Clinical Cancer Research* **2018**, *24* (11), 2539-2547.
- 25. Jokerst, J. V.; Lobovkina, T.; Zare, R. N.; Gambhir, S. S., Nanoparticle PEGylation for imaging and therapy. *Nanomedicine (London)* **2011**, *6* (4), 715-28.
- 26. Betley, T. A.; Banaszak Holl, M. M.; Orr, B. G.; Swanson, D. R.; Tomalia, D. A.; Baker, J. R., Tapping mode atomic force microscopy investigation of poly(amidoamine) dendrimers: effects of substrate and pH on dendrimer deformation. *Langmuir* **2001**, *17* (9), 2768-2773.
- 27. Hermanson, G. T., Chapter 2 Functional Targets for Bioconjugation. In *Bioconjugate Techniques (Third Edition)*, Hermanson, G. T., Ed. Academic Press: Boston, 2013; pp 127-228.
- 28. Makaraviciute, A.; Jackson, C. D.; Millner, P. A.; Ramanaviciene, A., Considerations in producing preferentially reduced half-antibody fragments. *Journal of Immunological Methods* **2016**, *429*, 50-56.
- 29. Myung, J. H.; Cha, A.; Tam, K. A.; Poellmann, M.; Borgeat, A.; Sharifi, R.; Molokie, R. E.; Votta-Velis, G.; Hong, S., Dendrimer-Based Platform for Effective Capture of Tumor Cells after TGFbeta1-Induced Epithelial-Mesenchymal Transition. *Anal Chem* **2019**, *91* (13), 8374-8382.
- 30. Izumi, S.; Yamamura, S.; Hayashi, N.; Toma, M.; Tawa, K. A.-O., Dual-color fluorescence imaging of EpCAM and EGFR in breast cancer cells with a bull's eye-type plasmonic chip. *Sensors (Basel)* **2017**, *17* (12), E2942.

- 31. Zhang, L.; Ridgway Ld Fau Wetzel, M. D.; Wetzel Md Fau Ngo, J.; Ngo J Fau Yin, W.; Yin W Fau Kumar, D.; Kumar D Fau Goodman, J. C.; Goodman Jc Fau Groves, M. D.; Groves Md Fau Marchetti, D.; Marchetti, D., The identification and characterization of breast cancer CTCs competent for brain metastasis. *Science Translational Medicine* **2013**, *5* (180), 180ra48.
- 32. Soares Martins, T.; Catita, J. A.-O.; Martins Rosa, I.; O, A. B. d. C. E. S.; Henriques, A. A.-O., Exosome isolation from distinct biofluids using precipitation and column-based approaches. *PLOS One* **2018**, *13* (6), e0198820.
- 33. Ratto, T. V.; Rudd, R. E.; Langry, K. C.; Balhorn, R. L.; McElfresh, M. W., Nonlinearly additive forces in multivalent ligand binding to a single protein revealed with force spectroscopy. *Langmuir* **2006**, *22* (4), 1749-57.
- 34. Sulchek, T.; Friddle, R. W.; Noy, A., Strength of multiple parallel biological bonds. *Biophysical Journal* **2006**, *90* (12), 4686-91.
- 35. Leistra, A. N.; Han, J. H.; Tang, S.; Orr, B. G.; Banaszak Holl, M. M.; Choi, S. K.; Sinniah, K., Force spectroscopy of multivalent binding of riboflavin-conjugated dendrimers to riboflavin binding protein. *The Journal of Physical Chemistry*. *B* **2015**, *119* (18), 5785-92.
- 36. Hummer, G.; Szabo, A., Free energy profiles from single-molecule pulling experiments. *Proceedings of the National Academy of Sciences of the United States of America* **2010**, *107* (50), 21441-6.
- 37. Leroueil, P. R.; DiMaggio, S.; Leistra, A. N.; Blanchette, C. D.; Orme, C.; Sinniah, K.; Orr, B. G.; Banaszak Holl, M. M., Characterization of folic acid and poly(amidoamine) dendrimer interactions with folate binding protein: a force-pulling study. *The Journal of Physical Chemistry*. *B* **2015**, *119* (35), 11506-12.